doi:10.1093/brain/awy253 BRAIN 2018: 141; 3144–3159 | 3144

BRAIN
A JOURNAL OF NEUROLOGY

LGI1 antibodies alter $K_v1.1$ and AMPA receptors changing synaptic excitability, plasticity and memory

Mar Petit-Pedrol,[1,*] Josefine Sell,[2,*] Jesús Planagumà,[1] Francesco Mannara,[1] Marija Radosevic,[1] Holger Haselmann,[2,3] Mihai Ceanga,[2] Lidia Sabater,[1] Marianna Spatola,[1,4] David Soto,[1,5] Xavier Gasull,[1,5] Josep Dalmau[1,6,7,8,#] and Christian Geis[2,3,#]

[*,#]These authors contributed equally to this work.

See Debanne and El Far (doi:10.1093/brain/awy271) for a scientific commentary on this article.

Leucine-rich glioma-inactivated 1 (LGI1) is a secreted neuronal protein that forms a trans-synaptic complex that includes the presynaptic disintegrin and metalloproteinase domain-containing protein 23 (ADAM23), which interacts with voltage-gated potassium channels $K_v1.1$, and the postsynaptic ADAM22, which interacts with AMPA receptors. Human autoantibodies against LGI1 associate with a form of autoimmune limbic encephalitis characterized by severe but treatable memory impairment and frequent faciobrachial dystonic seizures. Although there is evidence that this disease is immune-mediated, the underlying LGI1 antibody-mediated mechanisms are unknown. Here, we used patient-derived immunoglobulin G (IgG) antibodies to determine the main epitope regions of LGI1 and whether the antibodies disrupt the interaction of LGI1 with ADAM23 and ADAM22. In addition, we assessed the effects of patient-derived antibodies on $K_v1.1$, AMPA receptors, and memory in a mouse model based on cerebroventricular transfer of patient-derived IgG. We found that IgG from all patients (n = 25), but not from healthy participants (n = 20), prevented the binding of LGI1 to ADAM23 and ADAM22. Using full-length LGI1, LGI3, and LGI1 constructs containing the LRR1 domain (EPTP1-deleted) or EPTP1 domain (LRR3-EPTP1), IgG from all patients reacted with epitope regions contained in the LRR1 and EPTP1 domains. Confocal analysis of hippocampal slices of mice infused with pooled IgG from eight patients, but not pooled IgG from controls, showed a decrease of total and synaptic levels of $K_v1.1$ and AMPA receptors. The effects on $K_v1.1$ preceded those involving the AMPA receptors. In acute slice preparations of hippocampus, patch-clamp analysis from dentate gyrus granule cells and CA1 pyramidal neurons showed neuronal hyperexcitability with increased glutamatergic transmission, higher presynaptic release probability, and reduced synaptic failure rate upon minimal stimulation, all likely caused by the decreased expression of $K_v1.1$. Analysis of synaptic plasticity by recording field potentials in the CA1 region of the hippocampus showed a severe impairment of long-term potentiation. This defect in synaptic plasticity was independent from K_v1 blockade and was possibly mediated by ineffective recruitment of postsynaptic AMPA receptors. In parallel with these findings, mice infused with patient-derived IgG showed severe memory deficits in the novel object recognition test that progressively improved after stopping the infusion of patient-derived IgG. Different from genetic models of LGI1 deficiency, we did not observe aberrant dendritic sprouting or defective synaptic pruning as potential cause of the symptoms. Overall, these findings demonstrate that patient-derived IgG disrupt presynaptic and postsynaptic LGI1 signalling, causing neuronal hyperexcitability, decreased plasticity, and reversible memory deficits.

1 Institut d'Investigacions Biomèdiques August Pi i Sunyer (IDIBAPS), Hospital Clínic, Universitat de Barcelona, Barcelona, Spain
2 Hans-Berger Department of Neurology, Jena University Hospital, Jena, Germany
3 Center for Sepsis Control and Care (CSCC), Jena University Hospital, Jena, Germany
4 University of Lausanne (UNIL), Lausanne, Switzerland

Received March 12, 2018. Revised August 23, 2018. Accepted August 28, 2018. Advance Access publication October 20, 2018

5 Laboratori de Neurofisiologia, Departament de Biomedicina, Facultat de Medicina i Ciències de la Salut, Institut de Neurociències, Universitat de Barcelona, Barcelona, Spain
6 Department of Neurology, University of Pennsylvania, Philadelphia, USA
7 Centro de Investigación Biomédica en Red Enfermedades Raras (CIBERER), Valencia, Spain
8 Institució Catalana de Recerca i Estudis Avançats (ICREA), Barcelona, Spain

Correspondence to: Josep Dalmau, MD, PhD
IDIBAPS-Hospital Clínic, University of Barcelona, Casanova, 143; Floor 3ª, Barcelona 08036, Spain
E-mail: Jdalmau@clinic.cat

Correspondence may also be addressed to: Christian Geis, MD
Hans-Berger Department of Neurology, Jena University Hospital, Am Klinikum 1, 07747 Jena, Germany
E-mail: Christian.geis@med.uni-jena.de

Keywords: limbic encephalitis; LGI1; AMPA receptors; $K_v1.1$; synaptic hyperexcitability

Abbreviations: AMPAR = AMPA receptor; DTX = α-dendrotoxin; (e)EPSC = (evoked) excitatory postsynaptic current; fEPSP = field excitatory postsynaptic potential; LTP = long term potentiation

Introduction

Autoimmune encephalitides refer to a group of inflammatory brain diseases that manifest with prominent neuropsychiatric symptoms and are associated with antibodies against neuronal cell surface proteins, ion channels or receptors (Dalmau *et al.*, 2017). One of the most frequent types of autoimmune encephalitis predominantly affects the limbic system (limbic encephalitis) and can result from autoantibodies against different antigens, such as leucine-rich glioma-inactivated 1 (LGI1) protein, the α-amino-3-hydroxy-5-methyl-4-isoxazolepropionic acid receptor (AMPAR), the γ-aminobutyric acid (GABA) type B receptor, or contactin-associated protein-like 2 (Caspr2), each of them manifesting with a core syndrome that includes severe difficulty in forming new memories (anterograde or short-term memory deficit), changes of mood and behaviour, and variable presence of seizures (Dalmau and Graus, 2018). The most frequent is autoimmune limbic encephalitis with antibodies against LGI1 (Irani *et al.*, 2010; Lai *et al.*, 2010). Patients with this disorder often present with faciobrachial dystonic seizures or hyponatraemia that precede or develop together with the aforementioned core syndrome of limbic dysfunction (Irani *et al.*, 2013). Less frequently, patients with LGI1 antibodies present with rapidly progressive dementia which, as the other clinical manifestations, is responsive to immunotherapy (Arino *et al.*, 2016; Gadoth *et al.*, 2017).

Anti-LGI1 associated limbic encephalitis (or anti-LGI1 encephalitis) has an estimated incidence of 0.83 per 1 million individuals (van Sonderen *et al.*, 2016), strongly associates with DRB1*07:01-DQB1*02:02 and HLA-DRB4 (Kim *et al.*, 2017; van Sonderen *et al.*, 2017*b*), and rarely presents as a paraneoplastic manifestation of an underlying thymoma (van Sonderen *et al.*, 2017*a*). Different from other autoantigens of limbic encephalitis, which are synaptic receptors or cell membrane proteins, LGI1 is a secreted neuronal protein that has several binding partners, possibly organizing a trans-synaptic complex that includes the presynaptic disintegrin and metalloproteinase domain-containing protein 23 (ADAM23) and $K_v1.1$ potassium channels, and the postsynaptic ADAM22 and AMPAR (Sirerol-Piquer *et al.*, 2006; Fukata *et al.*, 2010). Mutations of LGI1 are linked to a disorder named 'autosomal dominant lateral temporal lobe epilepsy' (ADTLE), an inherited form of epilepsy characterized by partial seizures with acoustic or visual hallucinations (Poza *et al.*, 1999; Morante-Redolat *et al.*, 2002; Staub *et al.*, 2002). Several transgenic mouse models expressing a truncated LGI1 mutant that causes the inherited human disease, as well as LGI1 knock-out mice, showed an increase of excitatory synaptic transmission as compared with wild-type mice (Zhou *et al.*, 2009; Boillot *et al.*, 2016; Seagar *et al.*, 2017). These findings and evidence from experiments in oocytes after overexpression of $K_v1.1$, $K_v$beta1, LGI1, and mutated LGI1 (Schulte *et al.*, 2006) suggested that LGI1 decreases presynaptic release probability by upregulating presynaptic K_v1 channel activity *in vivo*. On the other hand, LGI1 knock-out mice also had decreased levels of postsynaptic AMPA receptor (AMPAR) in the hippocampal dentate gyrus (Ohkawa *et al.*, 2013).

A previous study examining the synaptic effects of patient-derived LGI1 antibodies showed that they disrupted the interaction of LGI1 with ADAM22 and reversibly reduced the postsynaptic clusters of AMPAR *in vitro* in rat hippocampal neurons (Ohkawa *et al.*, 2013). The antibodies also altered the interaction of LGI1 with a soluble construct of ADAM23 (Ohkawa *et al.*, 2013). An *in vitro* study using IgG from a single patient with antibodies against the voltage-gated K^+ channel complex (which includes LGI1) showed increased cell excitability in hippocampal brain slices (Lalic *et al.*, 2011). However, the antibody effects on $K_v1.1$ potassium channels and plasticity, and whether the patient's antibodies can impair memory were not reported. Considering the interaction of LGI1 with ADAM23, we reasoned that patient-derived antibodies would have a downstream effect on the $K_v1.1$ channels. Moreover, since anti-LGI1 encephalitis usually results in a treatable hippocampal dysfunction

characterized by difficulty in forming new memories (Arino *et al.*, 2016; van Sonderen *et al.*, 2016), we postulated that patient-derived antibodies would alter memory in a mouse model based on cerebroventricular transfer of the antibodies. Our findings reveal a complex pathogenic mechanism of LGI1 antibodies, involving both the $K_v1.1$ and AMPAR, and leading to alterations of plasticity and prolonged but reversible memory deficits.

Material and methods

Patient-derived serum samples

Serum samples of 25 patients with anti-LGI1 encephalitis were included in the assays (Supplementary Table 1). In all cases the presence of LGI1 antibodies was confirmed with rat brain tissue immunohistochemistry and a cell-based assay with human embryonic kidney (HEK)293 cells expressing LGI1 (Lai *et al.*, 2010). Serum samples from 20 antibody-negative healthy blood donors were used as controls. In a subset of experiments (field potential recordings) we additionally used CSF from patients and controls. Studies were approved by the institutional review board of Hospital Clínic and Institut d'Investigacions Biomèdiques August Pi i Sunyer (IDIBAPS), University of Barcelona and Jena University Hospital.

Serum IgG purification

Sera from eight high-titre LGI1 IgG antibody-positive patients with limbic encephalitis (presented in Supplementary Table 1) were pooled and the IgG (LGI1 IgG) isolated using agarose beads columns (#20423, Pierce), as reported (Gresa-Arribas *et al.*, 2016). IgG similarly isolated from pooled serum of antibody-negative healthy blood donors was used as control (control IgG). After IgG isolation, samples were dialyzed, normalized to a concentration of 4 μg/μl using Amicon Ultracentrifugal filters 30K (#UFC903024, Sigma-Aldrich), filtered, and kept at –80°C until use. The LGI1 specificity of the sample preparation was determined by immunohistochemistry with brain of LGI1 null mice, which showed lack of immunostaining (Supplementary Fig. 1); brain tissue from LGI1 null mice was kindly provided by J. K. Cowell (Yu *et al.*, 2010). Additional confirmation of the absence of brain-reacting antibodies other than anti-LGI1, was obtained by immunoabsorption of patient-derived LGI1 IgG with HEK293 cells expressing LGI1, which showed abrogation of reactivity of LGI1 IgG with brain tissue, cultured live neurons, and LGI1-expressing HEK293 cells (Supplementary material and Supplementary Fig. 2).

Production of soluble LGI1

HEK293 cells seeded in P100 dishes at a density of 2×10^6 cells were grown to a confluence of 70% and transfected with a human LGI1 plasmid (Origene, human sequence sc-116925) using Lipofectamine™ 2000 (Invitrogen) as reported (Lai *et al.*, 2010). Sixteen to 20 h after transfection, culture medium was replaced with reduced serum Opti-MEM™ medium (#51985-026, Gibco) and cells were incubated for 24 h at 37°C, 95% O_2, 5% CO_2. The medium was then collected and after adding protease inhibitors (1:50, #P8340, Sigma-Aldrich) it was concentrated (total protein, 3 mg/ml) using Amicon Ultracentrifugal filters 30K (#UFC903024, Millipore). The LGI1 enriched medium was then filtered through 0.22 μm polyvinylidene difluoride (PVDF) membrane filters (#sc-358812, Santa Cruz), and the presence of LGI1 in the media was determined by immunoblot using a polyclonal rabbit antibody against LGI1 (1:200, #ab30868, Abcam), as described in the Supplementary material. The same steps were carried out for the media of non-transfected HEK293 cells (used as control). The concentration of LGI1 in the media was determined by quantitative immunoblot comparing the LGI1 signal produced by the media with that produced by a commercially available LGI1 human recombinant protein of known concentration (#H00009211-P01, Abnova) (Supplementary material). These studies showed that the concentration of LGI1 in the enriched media was 4.2 μg/100 μl (Supplementary Fig. 3).

LGI1 deletion mutants

To identify the main epitope regions of LGI1, human full-length *LGI1* DNA (SC116925; NM_005097, Origene) in pCMV6-AC-GFP plasmid, and human *LGI3* DNA (Origene reference number RC213016) subcloned into pCMV6-AC-GFP plasmid, were used to generate deletion or chimeric constructs. In preliminary experiments a deletion construct containing the leucine-rich repeat domain of LGI1 (LRR1) was found to be recognized by all patients' antibodies, but a deletion construct containing the epitempin domain (EPTP1) was only recognized by 60% of the patients (data not shown). Considering the possibility that EPTP1 conformational epitopes could be lost by removing LRR1, we designed a construct in which LRR1 was replaced by the homologous LRR3 of LGI3, similar to that reported by Ohkawa *et al.* (2013). The cloning procedures were performed by GenScript, and four clones all containing the same signal peptide were used for the experiments: Clone 1 corresponded to the indicated human full-length *LGI1* DNA (LRR1-EPTP1); Clone 2 corresponded to the full-length *LGI3* DNA (LRR3-EPTP3); Clone 3 was a deletion construct that contained LRR1 (35–223 nucleotides), and Clone 4 contained LRR3 (31–220 nucleotides) and EPTP1 (224–557 nucleotides). To anchor the constructs to the cell membrane, all clones had the glycosylphosphatidylinositol (GPI) sequence of human *IGLON5* (RG225495; NM_001101372, Origene) added to the C-terminus; in addition, all clones had the green fluorescence protein (GFP) sequence added to the C-terminus (sequence obtained from the same commercially available IgLON5-GFP tagged plasmid). The presence of patient-derived serum antibodies

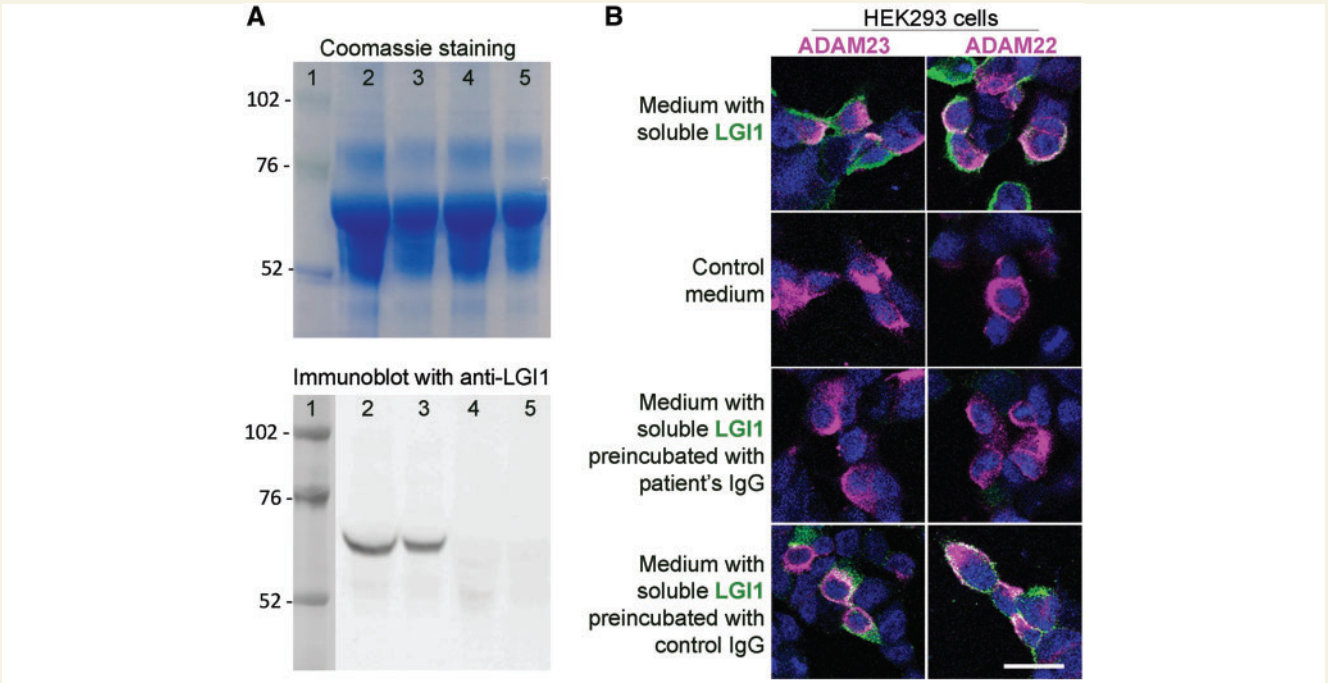

Figure 1 Patient's LGI1 IgG blocks the binding of soluble LGI1 to ADAM23 and ADAM22. (**A**) *Top*: Coomassie staining of proteins contained in the medium of HEK293 LGI1-expressing cells (lanes 2 and 3) and HEK293 cells not expressing LGI1 (lanes 4 and 5) (total protein load in lanes 2 and 4, 25 μg; and in lanes 3 and 5, 12.5 μg). *Bottom*: Immunoblot of protein preparations shown in the upper Coomassie panel using a polyclonal LGI1 antibody; note that LGI1 is only present in the medium derived from HEK LGI1-expressing cells. (**B**) HEK293 cells expressing ADAM23 or ADAM22 (in magenta) bind soluble LGI1 (in green) present in the medium of HEK293 cells expressing LGI1 (**B**, *top row*) but not present in control medium (**B**, *second row*). When the medium with soluble LGI1 is preincubated with a representative patient's LGI1 IgG the binding of LGI1 to ADAM23 or ADAM22 is abrogated (**B**, *third row*); in contrast, no blocking of the binding is observed when the medium is preincubated with control IgG (**B**, *fourth row*). Scale bar = 20 μm.

against each of these clones was determined with a conventional HEK293 cell-based assay, using serum dilutions 1:20 for 1 h at room temperature, and a secondary goat anti-human IgG Alexa Fluor® 594 (1:1000, A11014, Invitrogen) for 1 h.

LGI1 binding assay

Coverslips seeded with HEK293 cells at a 70% confluence were transfected with ADAM22 or ADAM23 [rat sequences containing a haemagglutinin (HA) tag] as reported (Lai *et al.*, 2010), and their expression was confirmed with a mouse polyclonal antibody against HA 6E2 (1:1000, #2367, Cell Signaling). To show that soluble LGI1 was able to bind to ADAM22 or ADAM23, coverslips with HEK293 live cells expressing ADAM22 or ADAM23 in 300 μl wells with Dulbecco's modified Eagle medium (DMEM) were exposed to the indicated LGI1 enriched medium (1:3 dilution or final LGI1 concentration, 1.4 μg/100μl) for 2 h at 37°C, washed with DMEM, and sequentially incubated for 45 min at 37°C with patient-derived LGI1 IgG or control IgG (1:50) and goat anti-human IgG Alexa Fluor® 488 (1:1000, #A11013, Invitrogen). A similar experiment was performed using goat polyclonal antibody against LGI1 (diluted 1:100, #sc9583, Santa Cruz) instead of human LGI1 IgG; in this setting the secondary antibody was donkey anti-goat Alexa Fluor® 488 (1:1000, #A11055, Invitrogen).

Parallel studies in which the indicated medium with soluble LGI1 had been preincubated with excess patient-derived or control IgG (total IgG concentration 2 mg/ml) for 2 h at 37°C, were used to determine whether patient-derived IgG interfered with the binding of soluble LGI1 to cells expressing ADAM22 or ADAM23.

Mice, placement of osmotic pumps, and behavioural tasks

Male C57BL6/J mice (Charles River), 8–10 weeks old (25–30 g) were used in the studies. Animal experiments were performed in accordance to the ARRIVE guidelines for reporting animal research (Kilkenny *et al.*, 2010) and the procedures were approved by the local ethics committee at the Universities of Barcelona and Jena. Detailed information on the animal studies including surgery, placement of ventricular catheters and osmotic pumps, and behavioural tests is provided as Supplementary material and has been previously reported (Planaguma *et al.*, 2015). The distribution of behavioural tests in relation to the infusion of LGI1 IgG or control IgG is shown in Supplementary Fig. 4. Overall, 143 mice were used for these studies: 83 for behavioural and brain tissue studies (quantification of

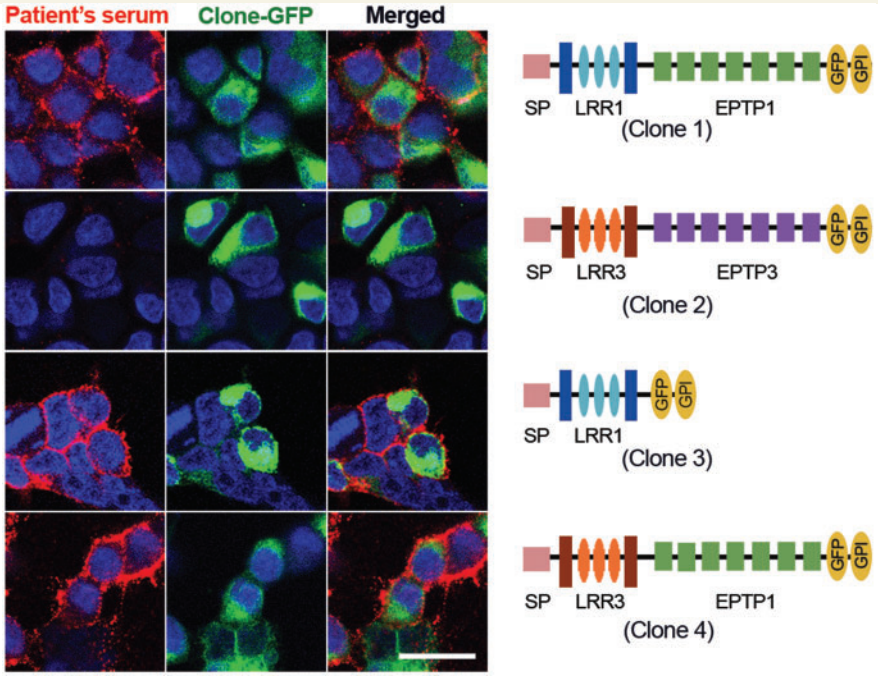

Figure 2 Reactivity of a patient's serum with deletion and chimeric constructs of LGI1. Serum from a representative patient with anti-LGI1 encephalitis shows predominant antibody reactivity (in red) with the full-length sequence of LGI1 (Clone 1), and the constructs that contain the LRR1 (Clone 3) and EPTP1 (Clone 4) domains. In contrast, the LRR3 and EPTP3 domains contained in the full-length LGI3 (Clone 2) were not recognized by patient's antibodies. Scale bar = 20 μm.

K_v1.1 and AMPAR clusters; antibody extraction; immunoprecipitation) and 60 for electrophysiological studies.

Immunofluorescence and confocal microscopy with brain tissue

Representative groups of mice were deeply anaesthetized with isoflurane, perfused with phosphate-buffered saline (PBS), and sacrificed at different time points (Days 1, 5, 13, 18, 26 and 47). The brains were removed and sagittally split into the two hemispheres. One hemisphere was fixed with 4% paraformaldehyde for 1 h, cryopreserved in 40% sucrose for 48 h, embedded in optimal cutting temperature compound (#4583, Tissue-Tek), and snap frozen in isopentane chilled with liquid nitrogen.

To determine the levels of presynaptic K_v1.1 potassium channels, 5-μm thick cryostat sections of brains were sequentially incubated with a polyclonal rabbit antibody against K_v1.1 (1:100, #ab32433, Abcam) for 2 h at room temperature, washed in PBS containing 0.3% Triton, and incubated with a mouse monoclonal antibody against the presynaptic marker Bassoon (1:250, #SAP7F407, Enzo), overnight at 4°C. Secondary antibodies included goat anti-rabbit Alexa Fluor® 488 and goat anti-mouse Alexa Fluor® 594 (both 1:1000, #A11008 and A11005, Invitrogen).

To determine whether the postsynaptic levels of AMPAR were affected, brain sections were incubated with a polyclonal guinea pig antibody against GluA1 (1:200, #AGP009, Alomone) for 2 h at room temperature, washed in PBS containing 0.3% Triton, and incubated with a rabbit polyclonal antibody against the postsynaptic marker PSD95 (1:250, #18258, Abcam) overnight at 4°C. Secondary antibodies included goat anti-guinea pig Alexa Fluor® 488, and goat anti-rabbit Alexa Fluor® 594 (1:1000, #A11073 and A11012, Invitrogen). The AMPAR that co-localized with PSD95 were defined as synaptic.

Total and synaptic clusters of the indicated proteins were visualized and quantified by confocal imaging (LSM710, Carl-Zeiss) using Imaris suite 7.6.4 (Bitplane), as reported (Planaguma *et al.*, 2015).

Acid-extraction of human antibodies from hippocampal tissue

The contralateral hippocampus of 14-day infused mice with LGI1 IgG or control IgG was dissected under a magnifying glass (Zeiss stereomicroscope, Stemi 2000), washed with cold PBS, homogenized in PBS containing a cocktail of protease inhibitors (1:50, #P8340, Sigma-Aldrich), and centrifuged at 16 000 rpm for 5 min. The supernatant was separated and kept as pre-extraction fraction; the pellet was resuspended in 0.1 M Na-citrate buffer pH 2.7 for 15 min on ice, centrifuged

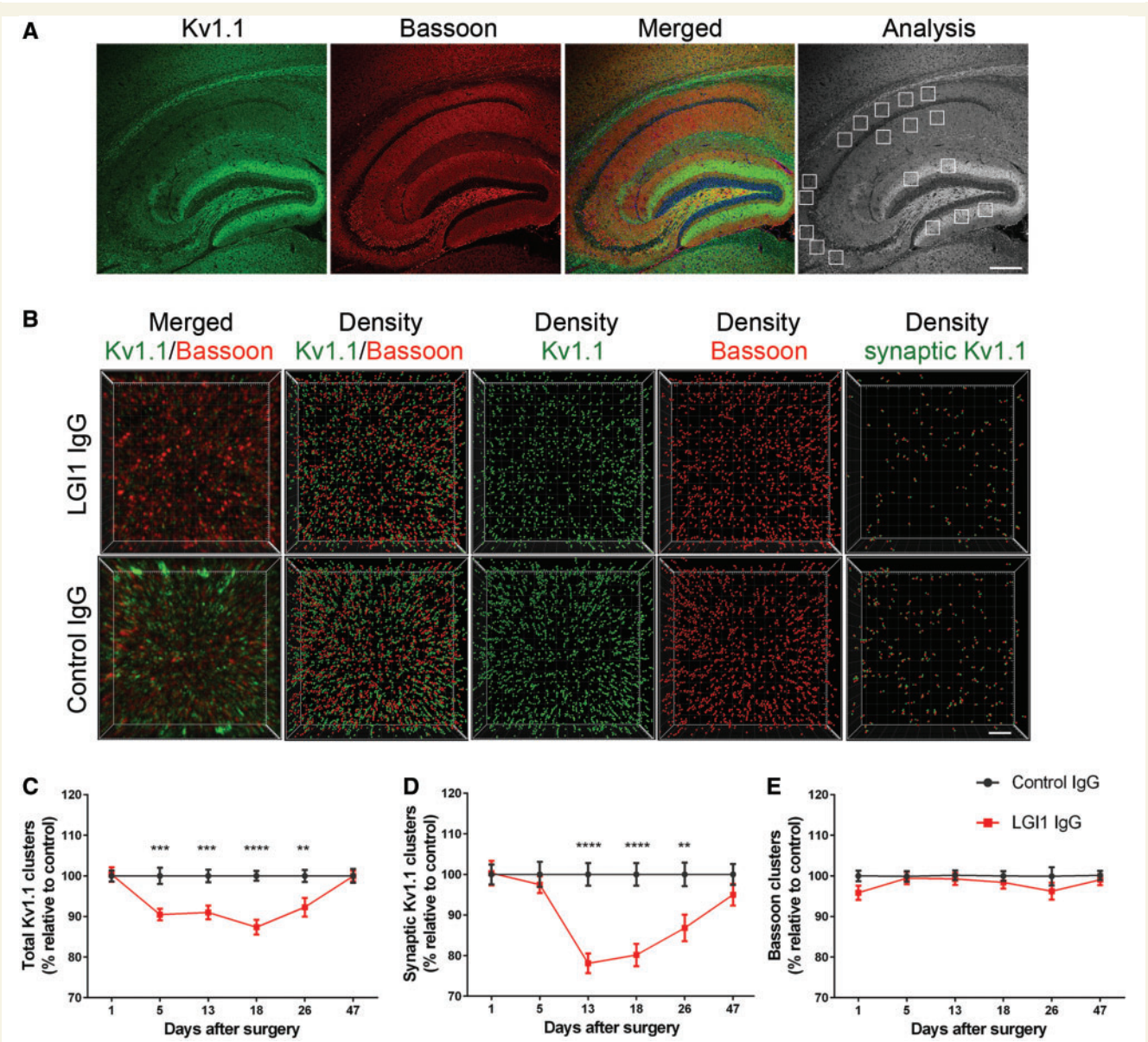

Figure 3 Patient-derived LGI1 IgG causes a decrease of total cell surface and synaptic $K_v1.1$ clusters in the hippocampus. (**A**) Sagittal section of hippocampus of a representative mouse infused with patient-derived LGI1 IgG demonstrating the immunostaining of $K_v1.1$, Bassoon, and the merging reactivities. Squares in 'Analysis' indicate the analysed subregions in CA1, CA3, and dentate gyrus for each animal. Scale bar = 200 μm. (**B**) 3D projection and analysis of the density of total clusters of $K_v1.1$ and Bassoon, and synaptic clusters of $K_v1.1$ (defined as $K_v1.1$ clusters that co-localized with Bassoon) in one of the indicated CA3 subregions (**A,** 'Analysis'). Merged images (**B**, *top and bottom left*; $K_v1.1$ green, and Bassoon red) were post-processed and used to calculate the density of the indicated clusters (density = spots/μm^3). Scale bar = 2 μm. (**C**–**E**) Quantification of the density of total (**C**) and synaptic (**D**) $K_v1.1$ clusters, and Bassoon clusters (**E**) in a pooled analysis of hippocampal subregions (CA1, CA3, dentate gyrus) in animals treated with patient-derived LGI1 IgG (red) or control IgG (black) on the indicated days. Mean density of clusters in control IgG treated animals was defined as 100%. Data are presented as mean ± SEM. For each time point five animals infused with patient-derived LGI1 IgG and five with control IgG were examined. Significance of treatment effect was assessed by two-way ANOVA with an alpha-error of 0.05 (asterisks) and *post hoc* testing with Sidak-Holm adjustment. $^{**}P < 0.01$, $^{***}P < 0.001$, $^{****}P < 0.0001$.

(16 000 rpm, 5 min), and the supernatant containing the acid-extracted human IgG was separated and neutralized with 1.5 M Tris buffer pH 8.8 (extraction fraction). The presence of human LGI1 antibodies in the pre-extraction and extraction fractions was assessed with the indicated HEK293-LGI1 cell-based assay (Lai *et al.*, 2010).

LGI1 immunoprecipitation from brain tissue

Representative mice brain from animals infused for 14 days with LGI1 IgG or control IgG were used for this experiment. Brains were removed, washed with PBS, the hippocampus

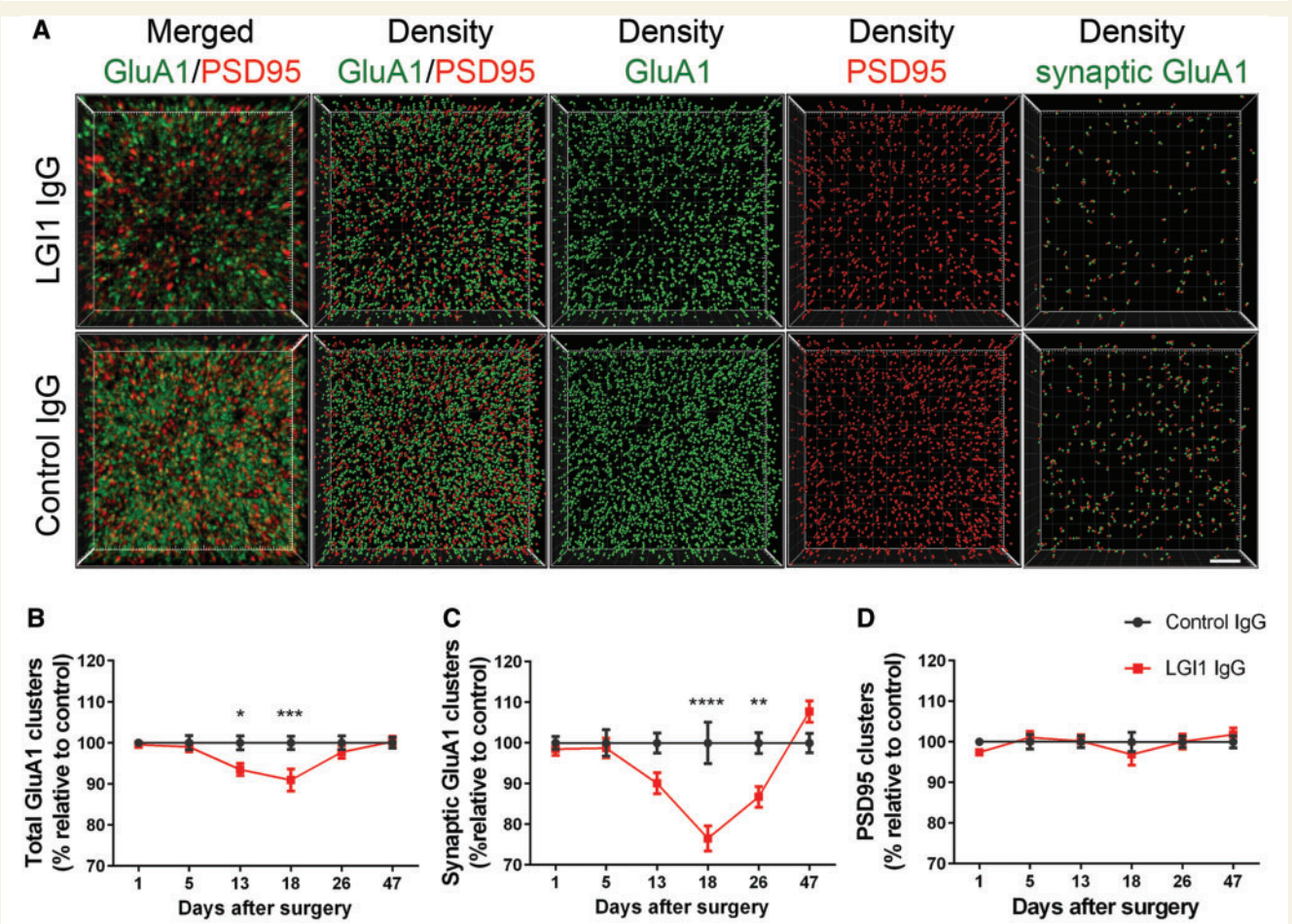

Figure 4 Patient-derived LGI1 IgG causes a decrease of total cell surface and synaptic AMPAR clusters in the hippocampus. (**A**) 3D projection and analysis of the density of total clusters of GluA1 AMPAR and PSD95, and synaptic clusters of AMPAR (defined as AMPAR clusters that co-localized with PSD95) in one of the CA3 subregions indicated in Fig. 3A, 'Analysis'. Merged images (**A**, *top and bottom left*; GluA1 green, and PSD95 red) were post-processed and used to calculate the density of the indicated clusters (density = spots/μm^3). Scale bar = 2 μm. (**B**–**D**) Quantification of the density of total (**B**) and synaptic (**C**) GluA1 AMPAR clusters, and PSD95 clusters (**D**) in a pooled analysis of hippocampal subregions (CA1, CA3, dentate gyrus) in animals treated with patient-derived LGI1 IgG (red) or control IgG (black) on the indicated days. Mean density of clusters in control IgG treated animals was defined as 100%. Data are presented as mean ± SEM. For each time point five animals infused with patient-derived IgG and five with control IgG were examined. Significance of treatment effect was assessed by two-way ANOVA with an alpha-error of 0.05 (asterisks) and *post hoc* testing with Sidak-Holm adjustment. *$P < 0.05$, **$P < 0.01$, ***$P < 0.001$, ****$P < 0.0001$.

dissected and homogenized with 500 μl of cold lysis buffer (NaCl 150 mM, EDTA 1 mM, Tris-HCl 100 mM, deoxycholic acid 0.5%, Triton™ X-100 1%) and a cocktail of protease inhibitors (1:50, #P8340, Sigma). After centrifugation (16 000 rpm for 20 min), the supernatant was retained and the IgG contained in the supernatant was precipitated with protein A/G agarose beads (100 μl beads; #20424, Thermo Fisher). The precipitated beads containing IgG were then washed five times with lysis buffer and after adding 25 μl of Rotiload (#K929.1, Roth) they were boiled for 5 min, centrifuged, and 25 μl of supernatant separated on a 4–12% Bis-Tris electrophoresis gel (#NP03222 NuPAGE®, Invitrogen), and transferred to a nitrocellulose membrane (#1704158, Bio-Rad). The presence of LGI1 in the IgG precipitate was demonstrated by blotting the membrane with a polyclonal rabbit antibody against LGI1 (1:200, #ab30868, Abcam) overnight at 4°C, followed by 1 h incubation with a peroxidase-labelled secondary anti-rabbit antibody (1:1000, GE HealthCare); the signal was developed with ECL western blotting detection reagent (#RPN2108, GE Healthcare) visualized with LAS4000 imager (GE Healthcare).

Electrophysiological recordings

Preparation of acute hippocampal brain slices was done 14–16 days after pump implantation. Mice were deeply anaesthetized, decapitated, and the brain was removed in ice-cold protective cutting artificial CSF [aCSF1 for patch-clamp recordings (in mM); 95 *N*-methyl-D-glutamine, 30 $NaHCO_3$, 20 HEPES, 25 glucose, 2.5 KCl, 1.25 NaH_2PO_4, 2 thiourea, 5 sodium ascorbate, 3 sodium pyruvate, 10 $MgSO_4$, 0.5 $CaCl_2$, 12 *N*-acetylcysteine, adjusted

to pH 7.3 and an osmolarity of 300 to 310 mOsmol, purged with 95% O_2/5% CO_2] (Grunewald *et al.*, 2017) or in high sucrose extracellular artificial fluid [aCSF2 for field potential recordings (in mM); 206 sucrose, 1.3 KCl, 1 $CaCl_2$, 10 $MgSO_4$, 26 $NaHCO_3$, 11 glucose, 1.25 NaH_2PO_4; purged with 95% CO_2/5% O_2, pH 7.4]. The brain was then subdivided into hemispheres and coronal hippocampal slices (300 µm for patch-clamp recordings and 380 µm for field potential recordings) were prepared on a vibratome (Leica VT1200 S).

Whole-cell patch-clamp recordings of dentate gyrus granule cells and CA1 pyramidal cells

Slices were incubated in aCSF1 at 34°C for 12 min and transferred into another incubation beaker with protective storage aCSF3 (in mM: 125 NaCl, 25 $NaHCO_3$, 25 glucose, 2.5 KCl, 1.25 NaH_2PO_4, 1 $MgCl_2$, 2 $CaCl_2$, 2 thiourea, 5 sodium ascorbate, 3 sodium pyruvate, 12 N-acetylcysteine, adjusted to pH 7.3 and an osmolarity of 300 to 310 mOsmol, purged with 95% O_2/5% CO_2) at room temperature for at least 1 h until recording.

Electrophysiological measurements were performed with a HEKA EPC-10 double patch-clamp amplifier with a sampling rate of 20 kHz. All recordings were filtered at 2.9 and 10 kHz using Bessel filters of the amplifier. For whole-cell patch-clamp recordings single slices were transferred into a recording chamber and continuously submerged with recording aCSF4 (in mM: 125 NaCl, 25 $NaHCO_3$, 25 glucose, 2.5 KCl, 1.25 NaH_2PO_4, 1 $MgCl_2$, 2 $CaCl_2$, purged with 95% O_2/5% CO_2) at room temperature (Haselmann *et al.*, 2015). Measurements were done on dentate gyrus granule cells and CA1 pyramidal neurons of the hippocampus at holding potentials of –70 mV. Patch pipettes were pulled from thick-walled borosilicate glass and filled with intracellular solution (in mM: 120 K-gluconate, 20 KCl, 10 HEPES, 0.1 EGTA, 4 Mg-ATP, 0.2 Na_2-GTP, 2 $MgCl_2$, 10 Na-phosphocreatine, adjusted to pH 7.3 with CsOH and an osmolarity of 280 mOsmol) and had a final resistance of 2.5–5 MΩ. Series resistance was compensated (70–80%) and monitored during the recordings. For evaluation of evoked excitatory postsynaptic currents (eEPSCs) in dentate gyrus granule cells the medial perforant path was stimulated by a theta glass bipolar electrode filled with aCSF4 and connected to a stimulus isolation unit (Isoflex, A.M.P.I). Supramaximal stimulation was determined when increasing stimulation did not result in an increase of eEPSC and ranged from 200 to 400 µA. For isolation of AMPAR-mediated glutamatergic transmission, 50 µM 2-amino-5-phosphonovalerate (AP-5, #0106, Tocris) and 20 µM bicuculline (#0109, Tocris) in aCSF4 perfusion were used to block NMDA receptors and GABAa receptors, respectively. For evaluation of minimally stimulated EPSCs in CA1 pyramidal neurons, minimal stimulation of the Schaffer collateral pathway was performed using a theta glass bipolar electrode (stimulation currents 7–19 pA) placed at least 200 µm from the recording site to avoid direct dendritic stimulation. Stimulation was systematically decreased until all-or-none unitary events with frequent initial failures were detectable and minimally-stimulated EPSC amplitude and failure rate was stable in a range of about 5% alteration of stimulation intensity (Stevens and Wang, 1995; Geis *et al.*, 2010; Lalic *et al.*, 2011). Under the condition of minimal stimulation in the Schaffer collateral pathway the majority of minimally stimulated EPSCs in CA1 pyramidal neurons derive from an individual synapse after fusion of a single vesicle (unitary event) (Stevens and Wang, 1995). Failures were visually identified and the failure rate was calculated as percentage of all trials. Peak amplitude calculation of minimally stimulated EPSCs was performed as averages of all trials excluding failures. In separate experimental groups, 100 nM α-dendrotoxin (DTX, #D-350, Alomone) was added >10 min before recordings to block K_v channels. Paired-pulse facilitation of EPSCs after supramaximal and minimal stimulation was measured with interstimulus intervals of 50 ms. Whole cell recordings were analysed by NeuroMatic plugin of Igor Pro Software 6 or 7 (Wavemetrics, Portland, OR, USA). Cells with series resistance >30 MΩ or series resistance changes of >20% during measurement were discarded. Liquid junction potential of 10 mV was corrected offline for all whole-cell patch clamp recordings.

Field potential recordings and analysis of long-term potentiation

Coronal hippocampal slices (380-µm thick) were transferred into an incubation beaker with aCSF5 (in mM: 119 NaCl, 2.5 KCl, 2.5 $CaCl_2$, 1.25 NaH_2PO_4, 1.5 $MgSO_4$, 25 $NaHCO_3$, 11 glucose, purged with 95% CO_2/5% O_2 pH 7.4). Slices were kept at 32°C for 60 min and subsequently at room temperature for at least 60 additional minutes. Slices were then transferred into a measurement chamber perfused with aCSF5 at 32°C. A bipolar stimulation electrode (Platinum-Iridium stereotrode, Science Products) was placed in the Schaffer collateral pathway (Planaguma *et al.*, 2016). Recording electrodes were made from borosilicate glass (BF150-86-10, Sutter Instruments). The recording electrode filled with aCSF5 was placed in the dendritic branching of the CA1 region for local field potential measurement (field excitatory postsynaptic potential, fEPSP). Signals were amplified and stored using AxoClamp 2B (Molecular Devices) or an HEKA EPC-10 double patch-clamp amplifier. A stimulus isolation unit A385 (World Precision Instruments) was used to elicit stimulation currents. Before baseline recordings, input-output curves were determined for each slice with stimulation currents ranging from 25 to 700 µA at 0.03 Hz. The stimulation current was adjusted for each recording to evoke fEPSP, which was at

half of its maximal evoked amplitude. After baseline recordings for 20 min with 0.03 Hz, long term potentiation (LTP) was induced by theta-burst stimulation (10 theta bursts of four pulses of 100 Hz with an interstimulus interval of 200 ms, repeated seven times with 0.03 Hz). After LTP induction, fEPSPs were recorded for additional 50 min with 0.03 Hz. Recordings with unstable baseline measurements (variations higher than 20% in baseline fEPSPs) were discarded. In separate recordings 100 nM DTX was added by bath perfusion.

The recordings were done and analysed using Axon pCLAMP Software (Molecular Devices, version 10.6) and Igor Pro Software 7. Slopes of all recordings were measured within 1–1.5 ms of the linear part of the rising fEPSP before it reaches the peak and the fibre volley. For determination of theta-burst stimulation induced LTP, mean slope values of fEPSPs after theta-burst stimulation until end of the recording were compared between the experimental groups.

Golgi–Cox staining, Sholl analysis and synaptic spine quantification

Morphological dendrite and spine analyses were performed in granule cells of the dentate gyrus and pyramidal neurons of the CA1 region from the contralateral brain hemisphere of mice used in neurophysiological recordings. Directly after removal, Golgi silver impregnation was conducted with the FD Rapid GolgiStain™ Kit (FD NeuroTechnologies) according to manufacturer's instructions. Dendritic complexity was assessed with the Sholl ring method, including analysis of total dendritic length, number of branch ends, and number of dendrites per branch order. Density of dendritic spines was analysed in tertiary branches of CA1 pyramidal neurons. Spines were subclassified (thin, mushroom, stubby, filopodia or branched) according to previous reports (McKinney, 2010). Detailed information on Golgi-Cox staining Sholl and dendritic spine analysis is provided in the Supplementary material.

Statistical analysis

Confocal cluster densities of GluA1, $K_v1.1$, PSD95, or Bassoon, and behavioural tests with multiple time points (NOR, LOC, RI, ANH) were analysed using two-way ANOVA. All behavioural paradigms with single time points (BW, EPM) were analysed with independent sample *t*-tests. *Post hoc* analyses for all experiments used Bonferroni correction for multiple testing.

Electrophysiological measurements of In-Out curves were analysed with two-way ANOVA followed by Holm-Sidak *post hoc* test. Group comparisons of independent recordings were made using two-tailed *t*-tests or one-way ANOVA with Bonferroni *post hoc* test. The alpha-level used to determine significance was $P < 0.05$. All tests were done using GraphPad Prism (Version 7) or SigmaPlot (Version 13.0). Mean values were presented with standard error of the mean (SEM).

Data availability

Raw data were generated at Idibaps-Hospital Clinic, University of Barcelona, and at the Hans-Berger Department of Neurology, Jena University Hospital. Derived data supporting the findings of this study are available from the corresponding authors upon reasonable request.

Results

Patient-derived LGI1 IgG prevents the binding of LGI1 to ADAM23 and ADAM22

To determine whether patient-derived LGI1 IgG recognized soluble LGI1 and prevented its binding to ADAM23 or ADAM22, HEK293 cells expressing each of these proteins were incubated with LGI1-enriched or control media. The presence of LGI1 in the media was first confirmed with immunoblot (Fig. 1A, lanes 2 and 3), and the binding of soluble LGI1 to ADAM23 or ADAM22 was demonstrated in HEK293 cells expressing each of these proteins incubated with soluble LGI1 followed by patient-derived LGI1 IgG (Fig. 1B) or a commercial LGI1 antibody (data not shown). Preincubation of soluble LGI1 with the serum of each patient with LGI1 antibodies, but not with control serum, abrogated the binding of LGI1 to ADAM23 and ADAM22 (Fig. 1B and Supplementary Fig. 5).

The target epitopes of patient-derived antibodies are distributed in the LRR and EPTP domains of LGI1

All patient-derived samples strongly reacted with Clone 1 (full-length *LGI1*) and Clones 3 and 4 that contained the LRR1 and EPTP1 domains, respectively. None of the samples recognized Clone 2 (LGI3), which contained the same signal peptide (SP) of the other clones and LRR3 and EPTP3 (Fig. 2). None of the 20 control sera showed reactivity with any of the four clones (data not shown). These findings indicate that patient-derived antibodies are specifically directed against epitopes located in the LRR and EPTP domains of LGI1.

Passive transfer of patient-derived LGI1 IgG causes a decrease of $K_v1.1$ potassium channels and AMPAR

In mice infused with patient-derived LGI1 IgG, but not those infused with control IgG, the presence of human LGI1 antibodies specifically bound to brain was demonstrated with two techniques: immunoprecipitation of LGI1

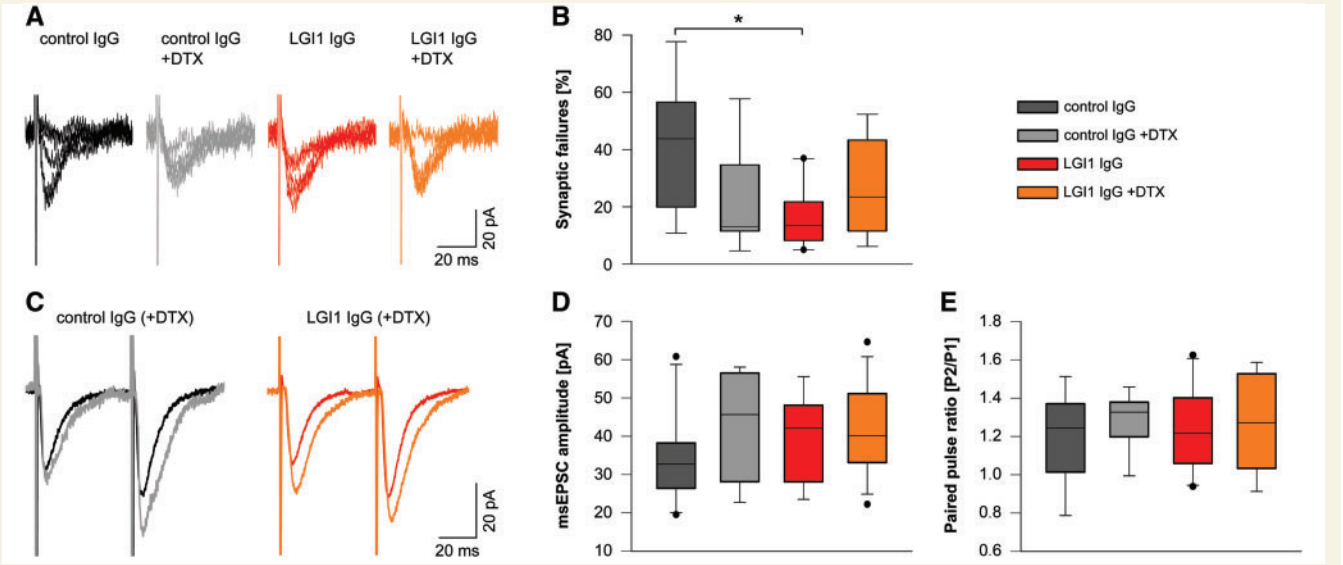

Figure 5 Patient-derived LGI1 IgG increases presynaptic release probability. (**A**) Example whole-cell recordings of unitary EPSCs of CA1 pyramidal neurons after minimal stimulation of Schaffer collateral axons. Five traces of the same cell are shown for each experimental group. (**B**) Failure rate of unitary events is decreased in neurons of LGI1 IgG treated mice similar to neurons of control IgG treated mice after application of DTX. Failure rate is unchanged in the LGI1 IgG group upon application of DTX ($n_{control\ IgG}$ = 8; $n_{control\ IgG+DTX}$ = 7; $n_{LGI1\ IgG}$ = 10; $n_{LGI1\ IgG+DTX}$ = 8; box plots show the median, 25th, and 75th percentiles; whiskers indicate the 10th and 90th percentiles, outlying points are depicted as dots; one-way ANOVA and Bonferroni *post hoc* test. *$P < 0.05$). (**C**–**E**) Peak amplitude of unitary minimally stimulated EPSCs (**D**) and paired pulse facilitation with an interstimulus interval of 50 ms (**E**) is similar in CA1 neurons of all experimental groups (synaptic failures are excluded). Exemplary average traces of individual cells are shown in **C**.

bound to patient-derived IgG using protein A/G agarose beads (Supplementary Fig. 6A), and acid-extraction of human antibodies bound to mouse brain, which showed to be LGI1-specific in a cell-based assay with LGI1-expressing HEK293 cells (Supplementary Fig. 6B).

To determine whether patient-derived LGI1 IgG altered the levels of K_v1.1 and AMPAR clusters, we focused on the hippocampus (Fig. 3A). This region was selected because anti-LGI1 encephalitis predominantly affects the hippocampus, which has close proximity to the lateral ventricles where the IgG fractions were infused. Compared with animals infused with control IgG, those infused with patient-derived LGI1 IgG had—on Days 13, 18 and 26—a significant decrease of the density of total and synaptic K_v1.1 clusters (Fig. 3B–D) followed by a gradual recovery after Day 26 (pooled analysis of the subregions in CA1, CA3, and dentate gyrus indicated in Fig. 3A). By contrast, patient-derived LGI1 IgG did not affect the density of the presynaptic marker Bassoon (Fig. 3E). The effect of patient-derived LGI1 IgG and control IgG on the levels of K_v1.1 in each subregion of the hippocampus is shown in Supplementary Fig. 7.

In parallel we investigated whether the levels of total and synaptic AMPAR (GluA1) clusters were altered in the same hippocampal areas examined in the K_v1.1 studies. The findings showed that mice infused with patient-derived LGI1 IgG had a decrease of total and synaptic AMPAR in the hippocampus (Fig. 4A–C). By contrast, LGI1 IgG did not alter the levels of the postsynaptic marker PSD95 (Fig. 4D). Considering each of the indicated subregions, the AMPAR changes were less prominent in CA3 than those observed with the K_v1.1 channels, and appeared to occur at mildly later time points, becoming significant on Day 18 in CA1 and in the dentate gyrus (Supplementary Fig. 8).

Patient-derived LGI1 IgG increases presynaptic excitability and glutamatergic synaptic transmission

To investigate the pathophysiological role of patient-derived LGI1 IgG in synaptic transmission, we examined the glutamatergic transmission by whole-cell patch-clamp recordings in the CA1 region and in the dentate gyrus of acute hippocampal slices of mice after the indicated 14-day cerebroventricular infusion of patient-derived LGI1 IgG or control IgG. We did not observe any differences in membrane properties, e.g. series resistance, resting membrane potential, or cell capacitance after 14-day infusion of LGI1 or control IgG in CA1 pyramidal neurons and dentate gyrus granule cells (not shown). We used minimal electrical stimulation of the Schaffer collateral pathway and whole-cell recordings of CA1 pyramidal cell EPSCs (minimally-stimulated EPSCs) to investigate monosynaptic transmission after single axon stimulation. We selected

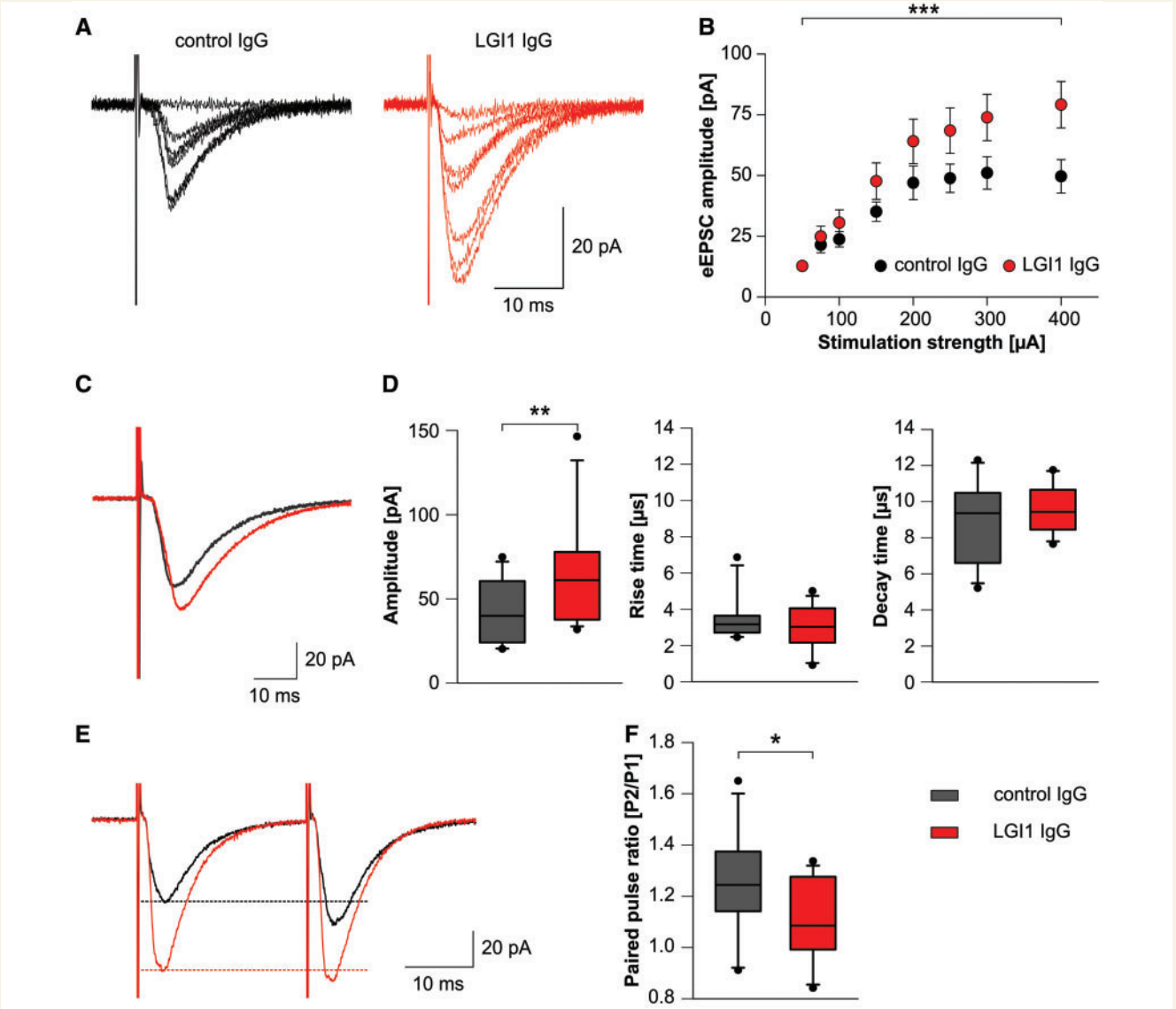

Figure 6 Patients' LGI1 IgG increases excitatory synaptic transmission. (**A** and **B**) Evoked excitatory postsynaptic currents (eEPSCs) in dentate gyrus granule cells upon incremental stimulation of medial perforant path (MPP) afferent fibres are increased in acute brain slices of mice that received patient-derived LGI1 IgG. Example traces of an individual recording are shown in **A**. In/out characteristics of granule cell neurons of control IgG and patient-derived LGI1 IgG treated mice (**B**; $n_{control\ IgG}$ = 13; $n_{LGI1\ IgG}$ = 15; data are presented as mean ± SEM; two-way ANOVA and Holm-Sidak *post hoc* test. ***$P < 0.001$). (**C** and **D**) Peak amplitude of eEPSCs (supramaximal stimulation; example traces in **C**) is increased after infusion of antibodies against LGI1, whereas rise and decay time is unchanged ($n_{control\ IgG}$ = 13; $n_{LGI1\ IgG}$ = 15; box plots show the median, 25th, and 75th percentiles; whiskers indicate the 10th and 90th percentiles, outlying points are depicted as dots; unpaired *t*-test. **$P < 0.01$). (**E** and **F**) Paired pulse facilitation with an interstimulus interval of 50 ms is reduced in granule cell neurons from mice after infusion of patient-derived LGI1 IgG indicating increased release probability. Example traces in **E**; dashed lines indicate peak amplitude of the first pulse ($n_{control\ IgG}$ = 11; $n_{LGI1\ IgG}$ = 13; box plots show the median, 25th, and 75th percentiles; whiskers indicate the 10th and 90th percentiles, outlying points are depicted as dots; unpaired *t*-test. *$P < 0.05$).

this pathway for minimal stimulation as under this condition most minimally-stimulated EPSCs represent fusions of a single vesicle (unitary event) (Stevens and Wang, 1995). For estimation of release probability, we analysed the failure rate of synaptic transmission after minimal stimulation. We found reduced synaptic failures in slices from mice infused with patient-derived LGI1 IgG. Failure rate in these slices was similar to slices of control IgG treated mice after superfusion with DTX, a specific blocker of K_v 1.1, 1.2, and 1.6 channels (Fig. 5A and B). Against to recordings in slices with control IgG, DTX application to slices from mice infused with patient-derived LGI1 IgG did not result in further reduction of the failure rate. Thus, treatment of mice with patient-derived LGI1 IgG resulted in similar increase of presynaptic release as compared to K_v1 blockade. When we analysed peak amplitude and

paired pulse facilitation of unitary minimally stimulated EPSCs after exclusion of synaptic failures we did not find changes in the experimental groups (Fig. 5C–E). Moreover, rise and decay time of these unitary events were unchanged (not shown). Considering that LGI1 strongly co-localizes with $K_v1.1$ in the middle molecular layer of the dentate gyrus (Schulte *et al.*, 2006), we recorded electrically-evoked EPSCs in the dentate gyrus granule cells of the hippocampus. Incremental stimulation of multiple axons in the medial perforant path from the entorhinal cortex led to increased peak amplitudes of eEPSCs at higher stimulus intensities in slices of mice infused with patient-derived LGI1 IgG as compared to control IgG, whereas eEPSC kinetics remained unchanged (Fig. 6A–D). This increase of excitatory synaptic transmission could either result from altered AMPAR formation on the postsynaptic density or from increased presynaptic release of glutamate, e.g. by increased release probability and axonal hyperexcitability. To determine whether short-term plasticity was altered in patient-derived LGI1 IgG treated mice after supramaximal stimulation, we performed paired-pulse recordings in the medial perforant path-granule cell pathway. Mice infused with patient-derived LGI1 IgG showed reduced paired-pulse facilitation as compared to control IgG infused mice indicating higher release probability (Fig. 6E and F). Together, these data suggest that mice with chronic infusion of LGI1-IgG have alterations in presynaptic function characterized by increased presynaptic excitability.

Patient-derived LGI1 IgG alters synaptic plasticity

Next, we examined synaptic plasticity in the hippocampus by recording field potentials (fEPSPs) in the CA1 pathway after stimulation of the Schaffer collateral in hippocampal slices of mice infused with patient-derived LGI1 IgG and control IgG. The findings showed impaired LTP in slices of mice infused with patient-derived LGI1 IgG as shown by reduced fEPSP slope values throughout the recording period up to 50 min after theta-burst stimulation (Fig. 7A and B). When we applied DTX to hippocampal slices of mice infused with patient-derived LGI1 IgG or control IgG, no additional changes in LTP were observed (Fig. 7A, C and Supplementary Fig. 9).

Dendritic pruning is unaffected by patient-derived LGI1 IgG

In a previous report using a transgenic mouse model with a truncated form of LGI1, abnormal dendritic pruning and increased spine density was associated with increased excitatory synaptic transmission (Zhou *et al.*, 2009). Here, we investigated dendritic pruning and spine morphology in mice infused with patient-derived LGI1 IgG and control IgG. Sholl analysis with concentric shells and neurolucida reconstructions of dentate gyrus granule cells showed unchanged dendritic arborization and dendrite length after infusion of patient-derived LGI1 IgG (Supplementary Fig. 10A–E). Analysis of synaptic spines in CA1 apical dendrites revealed identical spine density and unchanged spine morphology in both experimental groups (Supplementary Fig. 10F–H). Thus, changes in excitatory transmission and synaptic plasticity were not mediated by defective synaptic maturation.

Patient-derived LGI1 IgG causes memory deficits in mice

In parallel with the indicated effects of patient-derived LGI1 IgG on the levels of $K_v1.1$ and AMPAR, neuronal excitability and plasticity, mice infused with patient-derived IgG showed a progressive decrease of the object recognition index, indicative of a memory deficit (Bura *et al.*, 2007). The memory deficit became significant on Day 3 and persisted until Day 25 (11 days after the infusion of IgG had stopped). At the last time point (Day 47), the object recognition index had normalized and was similar to that of animals treated with control IgG (Fig. 8). Mice infused with control IgG only showed mild decline of initial memory performance that was not significant compared to baseline testing and may be caused by surgical procedures or non-specific effects of intraventricular IgG application. For all time-points, the total time spent exploring both objects (internal control) was similar in animals infused with patient-derived LGI1 IgG or control IgG (data not shown). No significant differences were noted in tests of anxiety (black and white test, elevated plus maze test), aggression (resident-intruder test) and locomotor activity (Supplementary Fig. 11).

Discussion

Previous clinical studies demonstrated that despite the severity of anterograde memory deficits, most patients with anti-LGI1 encephalitis improved with immunotherapy (Arino *et al.*, 2016; van Sonderen *et al.*, 2016; Gadoth *et al.*, 2017), and experimental studies showed that patient-derived antibodies caused a decrease of AMPAR in cultured neurons (Ohkawa *et al.*, 2013). These findings suggested the pathogenicity of LGI1 autoantibodies but the effects on an animal model were not investigated. Here we report a model based on cerebroventricular transfer of patient-derived IgG to mice showing that the antibodies alter the levels of $K_v1.1$ potassium channels and AMPAR causing a severe impairment of neuronal transmission, plasticity, and memory. These findings support a direct pathogenic role of patient-derived antibodies and suggest that similar mechanisms apply to the short-term memory deficit of the patients.

LGI1 is a neuronal secreted protein containing an N-terminal LRR-domain and a C-terminal EPTP domain (Fukata

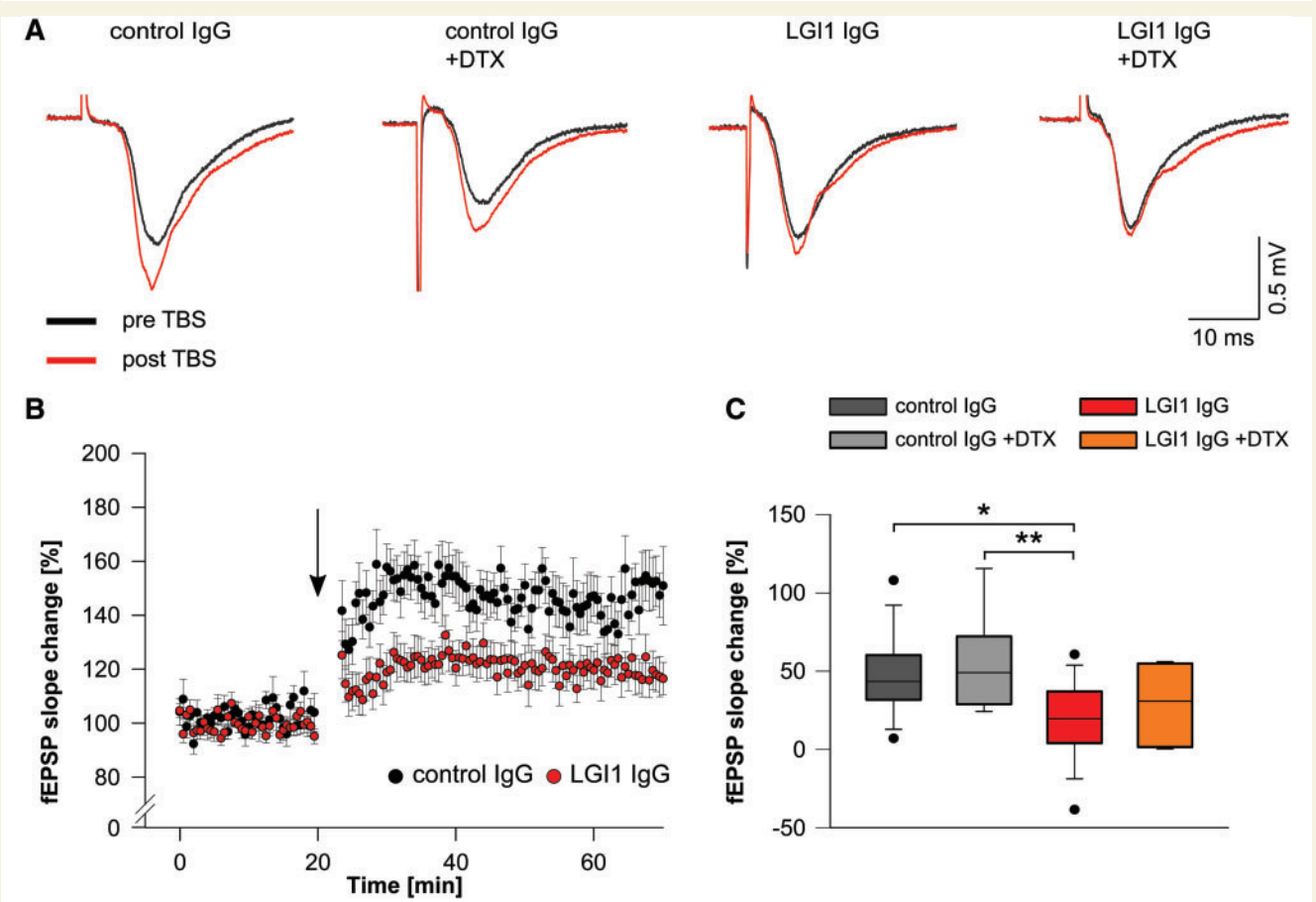

Figure 7 Patient-derived LGI1 IgG alters synaptic plasticity. (**A**) Example traces of individual fEPSP recordings in the CA1 region before (black traces) and after (red traces) theta burst stimulation (TBS) of Schaffer collateral afferents. Potentiation of fEPSPs is reduced in brain slices of mice that received patient-derived LGI1 IgG without further changes upon application of DTX. (**B**) Time course of LTP after theta-burst stimulation (arrow), demonstrates persistent reduction of fEPSP slope values in slices of mice after infusion of patient-derived LGI1 IgG indicating disturbed synaptic plasticity. (**C**) Quantification of fEPSP slope change is decreased in LGI1 IgG infused mice. Application of DTX does not alter fEPSP slope values in LGI1 and control IgG infused mice, respectively ($n_{\text{control IgG}}$ = 14; $n_{\text{control IgG+DTX}}$ = 9; $n_{\text{LGI1 IgG}}$ = 18; $n_{\text{LGI1 IgG+DTX}}$ = 8; box plots show the median, 25th, and 75th percentiles; whiskers indicate the 10th and 90th percentiles, outlying points are depicted as dots; one-way ANOVA and Bonferroni *post hoc* test. *P < 0.05, **P < 0.01).

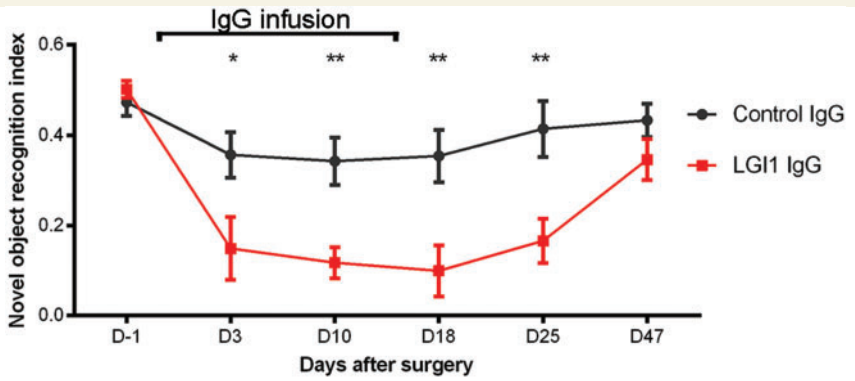

Figure 8 Cerebroventricular infusion of patient-derived LGI1 IgG causes decrease of memory. Novel object recognition index in mice treated with patient-derived LGI1 IgG (red, n = 16 mice) or control IgG (grey, n = 14 mice). A high index indicates better memory. Data are presented as mean ± SEM. *P < 0.05; **P < 0.01.

et al., 2006; Sirerol-Piquer *et al.*, 2006). Previous studies have shown that LGI1 interacts with the transmembrane metalloproteases ADAM23 and ADAM22 (Fukata *et al.*, 2006), which serve as receptors associated with presynaptic and axonal complexes containing $K_v1.1$ channels and postsynaptic complexes containing AMPAR, respectively. Using IgG fractions from 25 patients with anti-LGI1 encephalitis, we found that all patient-derived IgG strongly reacted with the LRR and EPTP domains of LGI1 and prevented the binding of LGI1 to ADAM23 and ADAM22, as previously shown by Ohkawa *et al.* (2013). These findings suggested that the effects of patient-derived antibodies did not only alter postsynaptic ADAM22 interactions, which include the AMPAR, but also presynaptic ADAM23 interactions, which include the $K_v1.1$ channels, as we demonstrate here in our animal model.

Mice with mutated or deficient LGI1 show a severe epileptic phenotype with premature death (Zhou *et al.*, 2009; Chabrol *et al.*, 2010; Fukata *et al.*, 2010; Yu *et al.*, 2010). In these genetic models, two potential underlying mechanisms have been reported including loss of synaptic AMPAR leading to reduction of AMPAR-mediated glutamatergic transmission (Fukata *et al.*, 2010; Lovero *et al.*, 2015), and defective function of axonal and presynaptic $K_v1.1$ resulting in enhanced excitatory transmission (Yu *et al.*, 2010; Boillot *et al.*, 2016; Seagar *et al.*, 2017). Here, after continuous intraventricular infusion of patient-derived LGI1 IgG, we found significant reduction of AMPAR and $K_v1.1$ clusters in the hippocampus, corroborating previous observations in LGI1 knockout mouse models (Fukata *et al.*, 2010; Lovero *et al.*, 2015; Seagar *et al.*, 2017). Moreover, in acute sections of hippocampus of mice infused with patient-derived LGI1 IgG, but not in those infused with control IgG, we found distinct functional evidence for hyperexcitability and enhanced glutamatergic transmission compatible with increased presynaptic release.

These findings are in agreement with a previous report showing increased firing frequency and enhanced excitability in CA3 neurons after preincubation of brain slices with IgG from patients with limbic encephalitis and antibodies against proteins of the voltage-gated K^+ channel complex (Lalic *et al.*, 2011), which presumably were directed against LGI1 (Lai *et al.*, 2010). It is known that presynaptic $K_v1.1$ potassium channel inactivation enhances release probability by increased and prolonged depolarization, Ca^{2+} influx, and subsequent potentiation of excitatory transmission (Geiger and Jonas, 2000). Indeed, recent studies in slice cultures or acute slices of LGI1 knockout mice showed evidence for enhanced neuronal excitability, increased release of presynaptic glutamate, and enlarged excitatory synaptic drive (Boillot *et al.*, 2016; Seagar *et al.*, 2017). In an oocyte expression system, LGI1 has been shown to prevent the N-type inactivation of $K_v1.1$ channels. Mutated LGI1 abrogated this effect, thus leading to rapid inactivation possibly contributing to an increase of action potential broadening and glutamate release (Schulte *et al.*, 2006).

The effect of patient-derived LGI1 IgG on synaptic plasticity was not mimicked by application of DTX in slices of hippocampus of mice infused with control IgG. Moreover, the application of DTX to slices of patient-derived LGI1 IgG treated mice did not further decrease LTP. Thus, the deterioration in synaptic plasticity upon chronic infusion of patient-derived IgG is most likely not mediated by changes in presynaptic $K_v1.1$ function but may be caused by insufficient synaptic incorporation of AMPAR during LTP as a result of disturbed trans-synaptic linker function of LGI1.

Together, in this model based on cerebroventricular transfer of patient-derived LGI1 IgG we identified several underlying pathophysiological mechanisms that are in good agreement with previous observations in LGI1 deficient model systems. Our findings point toward interference with LGI1 associated pathways that affect LGI1 signalling via post- and presynaptic mechanisms.

In our model we did not observe seizures, although electrographic recordings were not performed. Obviously, the degree of immune-mediated LGI1 disruption occurs gradually and is less pronounced to that of genetic LGI1 knockout models, which may be a reason why spontaneous seizures were not observed.

At the synaptic level the findings in the LGI1 deficient models as well as in the immune-mediated model make it difficult to explain how reduced AMPAR function associates with epileptic seizures in patients with ADTLE or anti-LGI1 encephalitis. Homeostatic downregulation of postsynaptic AMPAR in response to an ongoing presynaptic hyperexcitability has been proposed but it remains speculative and is not yet supported by experimental evidence (Seagar *et al.*, 2017). However, this hypothesis is in line with the observation that patient-derived LGI1 IgG caused a reduction of $K_v1.1$ expression (from Day 5 after onset of antibody infusion) that preceded the reduction of AMPAR clusters (from Day 13) in the hippocampus of infused mice.

In ADAM23 deficient mice (Owuor *et al.*, 2009) as well as in a transgenic model with truncated LGI1 (Zhou *et al.*, 2009), abnormal maturation of hippocampal synapses was observed. These changes consisted of a decrease of dendritic arborization in ADAM23 deficient mice, and a defective synaptic pruning with increased spine density in the transgenic mice. Different from these observations in germline knockout strains, application of LGI1 antibodies in adult mice did not induce changes in spine density or dendritic arborization. Furthermore, we did not detect any differences in neuronal membrane properties such as cell capacitance or input resistance. This is likely explained by the acute disturbance of LGI1 function by specific autoantibodies in the mature brain in contrast to chronic changes and adaptations in neuronal network following genetic mutation. Supporting these findings, a recent report revealed unchanged synaptic density and dendritic arborization in very young LGI1 knockout mice before onset of epileptic activity (Boillot *et al.*, 2016).

Overall, intraventricular application of patient-derived LGI1 IgG caused a decrease of levels of $K_v1.1$ and

AMPAR along with neuronal hyperexcitability and severe impairment of memory and plasticity; these findings are similar to those reported in models of genetic alteration of LGI1, supporting the pathogenicity of patient-derived LGI1 antibodies. Since LGI1 is a neuronal secreted linker protein, the antibody-mediated disturbance of this synaptic signalling pathway leads to fundamentally different pathophysiological mechanisms as compared with those associated with other antibody-mediated diseases, such as anti-NMDAR (Mikasova *et al.*, 2012; Planaguma *et al.*, 2015; Ladepeche *et al.*, 2018) or anti-AMPAR encephalitis (Haselmann *et al.*, 2018), where the antibodies alter the cell surface dynamics of the targets and cause their internalization. Interestingly, among the few antibody-mediated encephalitides that more frequently manifest as limbic encephalitis (Dalmau and Graus, 2018), two of them associate with antibodies that cause an important reduction of AMPAR, either by direct binding of the antibodies to the receptor (anti-AMPAR encephalitis) or by binding to synaptic partners, as shown here for LGI1. A task for the future is to clarify how antibody-binding to the protein-protein interaction domains of LGI1 (LRR, EPTP) affects LGI1 conformation and reactivity with its binding partners, and whether different approaches of antibody transfer (parenchymal, cortical) in different strains of mice lead to epileptic activity and seizures.

Acknowledgements

We thank Claudia Sommer (University of Jena, Germany), Esther Aguilar and Mercè Alba (Idibaps, University of Barcelona) for providing expert technical assistance in animal experiments, and John K Cowell (Augusta University, Augusta, GA, USA) for providing brain tissue of LGI1 null mice.

Funding

This work was supported by the Deutsche Forschungsgemeinschaft [CRC-TR 166 (TP B2) and GE2519_3-1 to C.G.]; by the IZKF and CSCC Jena to C.G.; Instituto Carlos III/FEDER (FIS PI14/00203, J.D.; PIE 16/00014, J.D.; FIS PI14/00141, X.G.; FIS PI17/00296, X.G.; RETIC RD16/0008/0014, X.G.), Fondation de l'Université de Lausanne et Centre Hospitalier Universitaire Vaudois (UNIL/CHUV), Lausanne, Switzerland (M.S.), NIH (RO1NS077851, J.D.), Ministerio de Economia, Industria y Competitividad, Spain (BFU2017-83317-P, D.S.), AGAUR (SGR93, J.D.; SGR737, X.G.), CERCA Programme / Generalitat de Catalunya), (PERIS) (SLT002/16/00346, J.P.), and Fundació CELLEX (J.D.).

Competing interests

The authors report no competing interests.

Supplementary material

Supplementary material is available at *Brain* online.

References

Arino H, Armangue T, Petit-Pedrol M, Sabater L, Martinez-Hernandez E, Hara M, et al. Anti-LGI1-associated cognitive impairment: presentation and long-term outcome. Neurology 2016; 87: 759–65.

Boillot M, Lee CY, Allene C, Leguern E, Baulac S, Rouach N. LGI1 acts presynaptically to regulate excitatory synaptic transmission during early postnatal development. Sci Rep 2016; 6: 21769.

Bura SA, Castane A, Ledent C, Valverde O, Maldonado R. Genetic and pharmacological approaches to evaluate the interaction between the cannabinoid and cholinergic systems in cognitive processes. Br J Pharmacol 2007; 150: 758–65.

Chabrol E, Navarro V, Provenzano G, Cohen I, Dinocourt C, Rivaud-Pechoux S, et al. Electroclinical characterization of epileptic seizures in leucine-rich, glioma-inactivated 1-deficient mice. Brain 2010; 133: 2749–62.

Dalmau J, Geis C, Graus F. Autoantibodies to synaptic receptors and neuronal cell surface proteins in autoimmune diseases of the central nervous system. Physiol Rev 2017; 97: 839–87.

Dalmau J, Graus F. Antibody-mediated encephalitis. N Engl J Med 2018; 378: 840–51.

Fukata Y, Adesnik H, Iwanaga T, Bredt DS, Nicoll RA, Fukata M. Epilepsy-related ligand/receptor complex LGI1 and ADAM22 regulate synaptic transmission. Science 2006; 313: 1792–5.

Fukata Y, Lovero KL, Iwanaga T, Watanabe A, Yokoi N, Tabuchi K, et al. Disruption of LGI1-linked synaptic complex causes abnormal synaptic transmission and epilepsy. Proc Natl Acad Sci USA 2010; 107: 3799–804.

Gadoth A, Pittock SJ, Dubey D, McKeon A, Britton JW, Schmeling JE, et al. Expanded phenotypes and outcomes among 256 LGI1/CASPR2-IgG-positive patients. Ann Neurol 2017; 82: 79–92.

Geiger JR, Jonas P. Dynamic control of presynaptic Ca(2+) inflow by fast-inactivating K(+) channels in hippocampal mossy fiber boutons. Neuron 2000; 28: 927–39.

Geis C, Weishaupt A, Hallermann S, Grunewald B, Wessig C, Wultsch T, et al. Stiff person syndrome-associated autoantibodies to amphiphysin mediate reduced GABAergic inhibition. Brain 2010; 133: 3166–80.

Gresa-Arribas N, Planaguma J, Petit-Pedrol M, Kawachi I, katada S, Glaser CA, et al. Human neurexin-3alpha antibodies associate with encephalitis and alter synapse development. Neurology 2016; 86: 2235–42.

Grunewald B, Lange MD, Werner C, O'Leary A, Weishaupt A, Popp S, et al. Defective synaptic transmission causes disease signs in a mouse model of juvenile neuronal ceroid lipofuscinosis. eLife 2017; 6: e28685.

Haselmann H, Mannara F, Werner C, Planaguma J, Miguez-Cabello F, Schmidl L, et al. Human autoantibodies against the AMPA receptor subunit GluA2 induce receptor reorganization and memory dysfunction. Neuron 2018, in press. doi: 10.1016/j.neuron.2018.07.048.

Haselmann H, Ropke L, Werner C, Kunze A, Geis C. Interactions of human autoantibodies with hippocampal GABAergic synaptic transmission - analyzing antibody-induced effects *ex vivo*. Front Neurol 2015; 6: 136.

Irani SR, Alexander S, Waters P, Kleopa KA, Pettingill P, Zuliani L, et al. Antibodies to K_v1 potassium channel-complex proteins leucine-rich, glioma inactivated 1 protein and contactin-associated protein-2 in limbic encephalitis, Morvan's syndrome and acquired neuromyotonia. Brain 2010; 133: 2734–48.

Irani SR, Stagg CJ, Schott JM, Rosenthal CR, Schneider SA, Pettingill P, et al. Faciobrachial dystonic seizures: the influence of immunotherapy on seizure control and prevention of cognitive impairment in a broadening phenotype Brain 2013; 136 (Pt 10): 3151–62.

Kilkenny C, Browne WJ, Cuthill IC, Emerson M, Altman DG. Improving bioscience research reporting: the ARRIVE guidelines for reporting animal research. PLoS Biol 2010; 8: e1000412.

Kim TJ, Lee ST, Moon J, Sunwoo JS, Byun JI, Lim JA, et al. Anti-LGI1 encephalitis is associated with unique HLA subtypes. Ann Neurol 2017; 81: 183–92.

Ladepeche L, Planaguma J, Thakur S, Suarez I, Hara M, Borbely JS, et al. NMDA receptor autoantibodies in autoimmune encephalitis cause a subunit-specific nanoscale redistribution of NMDA receptors. Cell Rep 2018; 23: 3759–68.

Lai M, Huijbers MG, Lancaster E, Graus F, Bataller L, Balice-Gordon R, et al. Investigation of LGI1 as the antigen in limbic encephalitis previously attributed to potassium channels: a case series. Lancet Neurol 2010; 9: 776–85.

Lalic T, Pettingill P, Vincent A, Capogna M. Human limbic encephalitis serum enhances hippocampal mossy fiber-CA3 pyramidal cell synaptic transmission. Epilepsia 2011; 52: 121–31.

Lovero KL, Fukata Y, Granger AJ, Fukata M, Nicoll RA. The LGI1-ADAM22 protein complex directs synapse maturation through regulation of PSD-95 function. Proc Natl Acad Sci USA 2015; 112: E4129–37.

McKinney RA. Excitatory amino acid involvement in dendritic spine formation, maintenance and remodelling. J Physiol 2010; 588 (Pt 1): 107–16.

Mikasova L, P DR Bouchet D, Georges F, Rogemond V, Didelot A, et al. Disrupted surface cross-talk between NMDA and Ephrin-B2 receptors in anti-NMDA encephalitis. Brain 2012; 135 (Pt 5): 1606–21.

Morante-Redolat JM, Gorostidi-Pagola A, Piquer-Sirerol S, Saenz A, Poza JJ, Galan J, et al. Mutations in the LGI1/Epitempin gene on 10q24 cause autosomal dominant lateral temporal epilepsy. Hum Mol Genet 2002; 11: 1119–28.

Ohkawa T, Fukata Y, Yamasaki M, Miyazaki T, Yokoi N, Takashima H, et al. Autoantibodies to epilepsy-related LGI1 in limbic encephalitis neutralize LGI1-ADAM22 interaction and reduce synaptic AMPA receptors. J Neurosci 2013; 33: 18161–74.

Owuor K, Harel NY, Englot DJ, Hisama F, Blumenfeld H, Strittmatter SM. LGI1-associated epilepsy through altered ADAM23-dependent neuronal morphology. Mol Cell Neurosci 2009; 42: 448–57.

Planaguma J, Haselmann H, Mannara F, Petit-Pedrol M, Grunewald B, Aguilar E, et al. Ephrin-B2 prevents N-methyl-D-aspartate receptor antibody effects on memory and neuroplasticity. Ann Neurol 2016; 80: 388–400.

Planaguma J, Leypoldt F, Mannara F, Gutierrez-Cuesta J, Martin-Garcia E, Aguilar E, et al. Human N-methyl D-aspartate receptor antibodies alter memory and behaviour in mice. Brain 2015; 138 (Pt 1): 94–109.

Poza JJ, Saenz A, Martinez-Gil A, Cheron N, Cobo AM, Urtasun M, et al. Autosomal dominant lateral temporal epilepsy: clinical and genetic study of a large Basque pedigree linked to chromosome 10q. Ann Neurol 1999; 45: 182–8.

Schulte U, Thumfart JO, Klocker N, Sailer CA, Bildl W, Biniossek M, et al. The epilepsy-linked Lgi1 protein assembles into presynaptic K_v1 channels and inhibits inactivation by $K_v$beta1. Neuron 2006; 49: 697–706.

Seagar M, Russier M, Caillard O, Maulet Y, Fronzaroli-Molinieres L, De San Feliciano M, et al. LGI1 tunes intrinsic excitability by regulating the density of axonal K_v1 channels. Proc Natl Acad Sci USA 2017; 114: 7719–24.

Sirerol-Piquer MS, Ayerdi-Izquierdo A, Morante-Redolat JM, Herranz-Perez V, Favell K, Barker PA, et al. The epilepsy gene LGI1 encodes a secreted glycoprotein that binds to the cell surface. Hum Mol Genet 2006; 15: 3436–45.

Staub E, Perez-Tur J, Siebert R, Nobile C, Moschonas NK, Deloukas P, et al. The novel EPTP repeat defines a superfamily of proteins implicated in epileptic disorders. Trends Biochem Sci 2002; 27: 441–4.

Stevens CF, Wang Y. Facilitation and depression at single central synapses. Neuron 1995; 14: 795–802.

van Sonderen A, Petit-Pedrol M, Dalmau J, Titulaer MJ. The value of LGI1, Caspr2 and voltage-gated potassium channel antibodies in encephalitis. Nat Rev Neurol 2017a; 13: 290–301.

van Sonderen A, Roelen DL, Stoop JA, Verdijk RM, Haasnoot GW, Thijs RD, et al. Anti-LGI1 encephalitis is strongly associated with HLA-DR7 and HLA-DRB4. Ann Neurol 2017b; 81: 193–8.

van Sonderen A, Thijs RD, Coenders EC, Jiskoot LC, Sanchez E, de Bruijn MA, et al. Anti-LGI1 encephalitis: clinical syndrome and long-term follow-up. Neurology 2016; 87: 1449–56.

Yu YE, Wen L, Silva J, Li Z, Head K, Sossey-Alaoui K, et al. Lgi1 null mutant mice exhibit myoclonic seizures and CA1 neuronal hyperexcitability. Hum Mol Genet 2010; 19: 1702–11.

Zhou YD, Lee S, Jin Z, Wright M, Smith SE, Anderson MP. Arrested maturation of excitatory synapses in autosomal dominant lateral temporal lobe epilepsy. Nat Med 2009; 15: 1208–14.